Experimental Investigation and Modeling of CO_2 Adsorption Using Modified Activated Carbon

Karbalaei Mohammad, Niyousha
Department of Chemistry, North Tehran Branch,
Islamic Azad University, P.O. Box 1651153311 Tehran, I.R. IRAN

Ghaemi, Ahad*[+]
School of Chemical, Petroleum and Gas Engineering, Iran University of Science and Technology,
P.O. Box 16765-163 Tehran, I.R. IRAN

Tahvildari, Kambiz; Sharif, Amir Abdollah Mehrdad
Department of Chemistry, North Tehran Branch,
Islamic Azad University, P.O. Box 1651153311 Tehran, I.R. IRAN

ABSTRACT: *In this research, Activated Carbon (AC) was modified using a sodium hydroxide solution for CO_2 adsorption. Adsorption experiments were carried out in a batch reactor at a temperature range of 20-80°C and a pressure range of 2-10 bars to investigate kinetic, isotherm, and thermodynamic of the CO_2 adsorption process. Activated carbon was modified with NaOH solution concentration in the range of 10-40%. Response Surface Methodology (RSM) was used to assess the combined effect of adsorption CO_2 pressure and temperature on CO_2 adsorption capacity. Also, RSM was used to obtain the optimum operational conditions. The results showed that modified activated carbon with 30% NaOH concentration (30SH-AC) provided the best performance for CO_2 adsorption. The optimum CO_2 adsorption capacity was obtained 104.32 mg/g for 30SH-AC at a temperature of 20°C and pressure 6 bars. The sips model was found to be the best for fitting the CO_2adsorption isotherm. Also, the kinetic study indicated that the pseudo-second-order model is well-fitted with the experimental data. The thermodynamics parameter shows that the CO_2 adsorption process is exothermic.*

KEYWORDS: *CO_2 Adsorption; NaOH; Modified activated carbon; Isotherm; Kinetic; Thermodynamic.*

INTRODUCTION

Generally, the main approaches to the removal of CO_2 are restricted to cryogenic distillation, membrane purification, absorption with solutions, and adsorption using solids [1-4]. Although cryogenic distillation is widely used in gas separation, this technique is likely to be ruled out in the case of CO_2 due to the high energy demand involved. Membranes are an efficient mass-separating agent for bulk separations. However,

***** *To whom correspondence should be addressed.*
+ E-mail: aghaemi@iust.ac.ir
1021-9986/2020/1/177-192 *16/$/6.06*

when CO_2 is a minor component as in the flue gases, membranes have reduced efficiency and are difficult to scale up [5-8].

Absorption with chemical solutions is the most mature technology for large-scale CO_2 capture using aqueous alkylamine solutions like monoethanolamine (MEA) and Diethanolamine (DEA) or other fluids with the basic character [9-13]. However, there are some problems associated with this technique, such as high equipment corrosion, high energy consumption in regeneration, oxidative degradation of absorbents, and loss of effectiveness over time due to low thermal stability and foaming in the gas-liquid interface [14-17].

Adsorption in porous solid materials such as activated carbon is an attractive alternative technology to overcome the techno-economical limitations of the above-mentioned technologies. Adsorption is a widely used technology for gas treatment due to its versatility and efficiency. Overall, adsorption of CO_2 by solid adsorbents is applied method due to its high CO_2 adsorption capacities, suitable for batch and continuous processes, high possibility of regeneration and potential reuse, and low energy requirement [18-21]. Various adsorbents such as inorganic-porous materials, activated carbons, basic oxide and amine-based have been employed in catalysis and adsorption of CO_2. But some of these adsorbents like the amine-based require high energy and possess degradation threat through oxidation that results in corrosion [22-26]. Carbon-based materials have high chemical and thermal stability as well as high adsorption capacities. Their low cost and recyclability make them ideal for gas pollutions prevention. Activated carbon as a highly microporous material with a large surface area has been recognized as one of the carbon-based materials for removing gas phase pollutants [18, 22]. In recent years, modification of activated carbon was carried out with KOH, NaOH, phosphoric acid to functionalization and improving surface area. Impregnation with sodium hydroxide (NaOH) is more effective in the modification of activated carbon because NaOH is inexpensive, minimally corrosive and environmentally friendly.

Tan et al. (2014) investigated CO_2 adsorption capacity on modified coconut shell activated carbon at different adsorption temperatures, including 35 °C, 45 °C and 55 °C and showed that a 32% NaOH concentration with a 3 h dwelling time provided the best CO_2 adsorption capacity [18]. Another study by Buczek.(2016) showed that process reactivation of carbon changes its particle size as well as density properties and increases by nearly twice the amounts of CH_4 and CO_2 adsorbed under high-pressure conditions [27]. *Guo et al.* (2006) studied the adsorption of CO_2 on a raw activated carbon A and three modified activated carbon samples B, C, and D at temperatures ranging from 29.85 to 59.85 °C and showed that the active ingredients impregnated in the carbon samples show significant influence on the adsorption for CO_2. The volumes adsorbed on modified carbon samples B, C, and D are all larger than that on the raw carbon sample A. On the other hand, the physical parameters such as surface area, pore volume, and micropore volume of carbon samples show no influence on the adsorbed amount of CO_2 [28]. *Shahkarami et al.* (2015) studied the effects of different activation techniques on CO_2 adsorption performance at temperature range of 25 to 65 °C. The results revealed that KOH activated carbon with a total micropore volume of 0.62 cm^3/g and surface area of 1400 m^2/g had the highest CO_2 adsorption capacity due to its microporous structure [29]. Another study by Sreńscek-Nazzal, et al. (2016) demonstrated that the AC modified with KOH had the highest S_{BET}, V_{tot}, V_{mic} values of 2063 m^2/g, 1.13 cm^3/g, and 0.67 cm3/g, respectively and the maximum CO_2 adsorption was 14.44 mmol/g for DTO/KOH modified carbon whereas 8.07 mmol/g of CO_2 was adsorbed at DTO [30]. The operating conditions of summarized studies on the CO_2 adsorption with modified activated carbon are presented in Table 1.

In the current research, the prepared activated carbon was modified to improve the CO_2 adsorption capacity by promoting NaOH on the surface of the activated carbon through chemical impregnation. CO_2 adsorption on a low cost and abundantly available adsorbent activated carbon modified with NaOH solution is evaluated at different operational conditions. Besides, the CO_2 adsorptions modeling including isotherm, kinetic and thermodynamic were investigated to determine the process behavior and the model's parameters. Also, response surface methodology was used to obtain the optimum operational conditions.

THEORITICAL SECTION

Adsorption Experiments with activated carbon and modified activated carbon by NaOH solutions

Table 1: Some of recent studies on the CO_2 adsorption with modified activated carbon.

Adsorbent	Input Gas Composition	T(°C)	Percentage of modifier	Method	Adsorption capacity				Ref.
- Activated Carbon (AC) - NaOH-Activated Carbon (30SH-AC)	CO_2	20 35 50 65 80	Modified with 10%,20%,30% ,40%	Batch Reactor	Adsorption capacity mg/g at 6 bar				Present Work
					AC	30SH-AC			
					56.89	104.32			
					28.76	60.98			
					9.80	30.57			
					7.8	19.35			
					5.80	12.55			
NaOH-Granular Coconut Shell AC	10%,15%,20 % CO_2 with N_2	35 45 55	Modified with 24%, 32% 40%, 48%	Fixed-Bed Reactor	Adsorption capacity mg/g				[18]
					27.10 24.03 16.62				
Active Carbon-KOH	CO_2-CH_4		Picazine Carbon / KOH ratio 1 : 3 (m/m)	PSA method					[27]
A)Activated Carbon B)AC-KOH C)AC-mixture of ethylenediamine & ethanol D)AC- mixture of KOH/ethylenediamine/ ethanol	CO_2	29.85 39.85 59.85	KOH 4% Mixture ethylenediamine & ethanol (2:1)	Glass vacuum system	A V_0 (ml_{STP}/g)	B V_0 (ml_{STP}/ g)	C n	D n	[28]
					9.096 8.292 7.830	14.769 14.288 12.761	2.61 2.43 2.47	2.33 2.52 2.26	
KOH-AC CO_2-AC Steam-AC	10-30 mol% CO_2 with He	25-65	Carbon to KOH mass ratio: 0.81	Fixed-Bed reactor	The highest adsorption capacity In 30mol% CO_2 / 25 °C (mg/g)				[29]
					KOH-AC	78			
					CO_2-AC	63			
					Steam-AC	59			
DTO (Commercial activated carbon) DTO-KOH DTO-$ZnCl_2$ DTO-K_2CO_3	CO_2	40	The mass ratio DTO:KOH is 1:3		Adsorption capacity mmol/g				[30]
					DTO	8.07			
					DTO-KOH	14.44			
					DTO-ZnCl2	9.15			
					DTO-K_2CO_3	8.70			

were carried out in a batch reactor. In the experiments, the influence of various parameters such as adsorbent dosage, contact time, temperature and pressure were studied. The reaction mechanism of carbon dioxide with the hydroxides has been proposed (Eq. (1)) as follows [31]:

$$2MOH(s)+CO_2(g)\rightarrow M_2CO_3(s)+H_2O(g) \quad (1)$$

Where $M=Na^+$. In the carbonation reaction, CO_2 is captured by carbonation adsorbent. The adsorption capacity of the adsorbent was calculated through the following equation Eq. (2) [32]:

$$q_e=\frac{(P_i-P_e)VM_{CO2}}{RTm}.10^3 \quad (2)$$

The adsorption percentage of adsorbent was calculated using Eq. (3):

$$\text{Adsorption}(\%)=\frac{P_i-P_e}{P_i}\times 100 \quad (3)$$

The correlation coefficient (R^2) was also used to determine the best-fitting models to the experimental data, illustrated as Eq. (4).

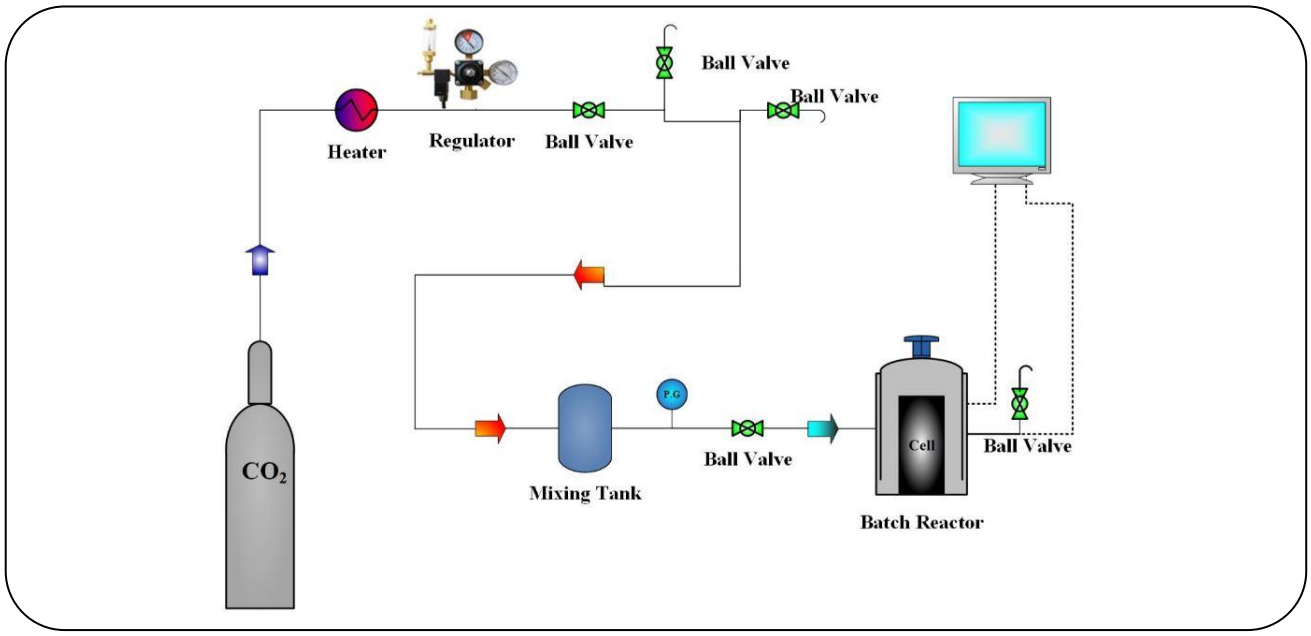

Fig. 1: Schematic of the experimental CO_2 adsorption set-up.

$$R^2 = \frac{\sum\left(q_m - \overline{q_e}\right)^2}{\sum\left(q_m - \overline{q_e}\right)^2 + \sum\left(q_m - q_e\right)^2} \quad (4)$$

EXPERIMENTAL SECTION

Materials

Commercial granular activated carbons of 0.5-2.2 mm particle sizes were purchased from the Iranian market. Sodium hydroxide (NaOH) with 99% purity was prepared from Merck chemical company (Germany). Also CO_2 gas was provided by Sabalan Gas Co. (Tehran, Iran) with purity of 99.98% and used as adsorbate gas without further purification.

Adsorption Set-up

CO_2 adsorption was performed in a stainless steel batch reactor. The schematic diagram of the experimental setup is shown in Fig. 1. To achieve better temperature control, which is essential for experiments, the reactor temperature was controlled using a cascade controller. Cell volume was estimated using the water displacement method [33]. The gas chamber volume was 160 cm^3. The reactor was loaded with 2 gr of adsorbent, and then the operating pressure and temperature were adjusted. The adsorbed amount was calculated using the non-ideal gas law, by measuring the pressure drop caused by CO_2 adsorption. The experiment was repeated with different parameters, such as varying pressures ranging from 2-10 bars at a temperature range of 20-80°C, to optimize the adsorption conditions.

Preparation of modified Adsorbent

Commercial granular activated carbon was modified by sodium hydroxide (NaOH) impregnation. For this aim, 30 g of activated carbon was treated with 100 mL of different concentration (10-40%) of NaOH solution and allowed to dwell for 24 h at room temperature. Then, the samples were dried in an oven at 105°C for 6 h. The prepared samples were named according to the used percentage of NaOH as 10SH-AC, 20SH-AC, 30SH-AC, and 40SH-AC for 10%, 20%, 30% and 40% NaOH, respectively. The prepared NaOH-modified activated carbons were later used as adsorbents to investigate their performance for CO_2 adsorption as shown in Table 2 and Fig. 2. As can be seen, the adsorption of CO_2 using 30% NaOH modified activated carbon (30SH-AC) gave the highest adsorption capacity. The unmodified AC can adsorb 56.89 mg/g CO_2, whereas the 10%, 20%, 30% and 40% NaOH modified adsorbents can adsorb79.362, 88.116, 104.319, and 80.635 mg/g CO_2, respectively. It revealed that modification of activated carbon with NaOH up to 30% had positive effect and dramatically increased the CO_2 absorption capacity. Also the result showed that 40SH-AC gave lower adsorption capacity

Table 2: Effect of NaOH concentration percentage on CO_2 adsorption capacity at 20 ℃ and 6 bars.

NaOH Concentration (%)	Adsorption Capacity (mg/g)
0	56.893
10	79.362
20	88.116
30	104.319
40	80.635

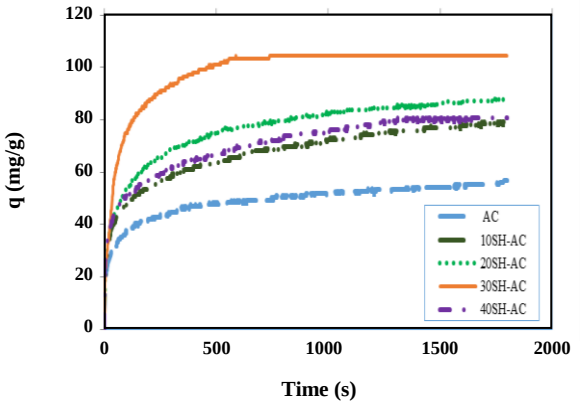

Fig. 2: Effect of NaOH concentration percentage on CO_2 adsorption capacity at 20 ℃ and 6 bars.

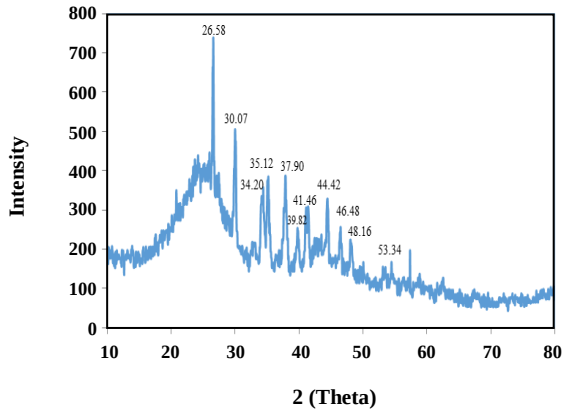

Fig. 3: XRD spectrum of 30SH-AC.

than 30SH-AC which can be related to filling pores and cavities of the adsorbent due to the excess concentration of NaOH solution, which leads to the decrease of CO_2 absorption capacity [18]. Since 30SH-AC showed the best performance for CO_2 adsorption, thus it was used for further studies.

Characterization of adsorbents

The Activated Carbon (AC) and 30SH-AC surface area and porosity were measured by Brunauer–Emmett–Teller (BET) technique using nitrogen adsorption/desorption isotherms determined at 77 K by a BELSORP-mini II analyzer. Samples were degassed at 300 °C for 2 h measurement of equilibrium pressure of a known volume of liquid nitrogen for the generation of adsorption–desorption isotherms. FT-IR analysis was performed using an FT-IR spectrometer (Thermo, Model Nicolet 8700 FTIR, USA) to identify the surface functional groups on the AC and 30SH-AC. In addition, X-ray diffraction (XRD) pattern of adsorbent was obtained on an X-ray diffractometer (Philips PW1730) using Cu Kα radiation (k=1.54 A°). The XRD diffractogram of 30SH-AC is shown in Fig. 3. As can be seen in Fig. 3, the sharp peak around 26.58 degree reveals the presence of carbon and dispersion peaks in the values of 30.07, 34.20, 35.12, 37.90,39.82, 41.46, 44.42, 46.48,48.16 and 53.34 degrees signify the formation of Na_2CO_3 which indicate the reaction (1) has been carried out.

The BET quantitative analysis for surface area and porosity of AC and 30SH-AC are presented in Table 3. The values of the BET surface area and mean pore diameter after modification by 30% NaOH decreased compared to the AC which were attributed to the structural changes of the adsorbent because of entrapment of NaOH in the micropore area, which reduced the final surface area of the adsorbent.

The FTIR spectrum of the adsorbent is important for evaluating the active functional groups on the surface of the raw material and on the adsorbent. The spectra of the AC and 30SH-AC before and after CO_2 adsorption are displayed in Fig. 4. All of the FTIR curves were similar. The broad stretches around 3433.44, 3424.66 and 3427.94 cm^{-1} respectively, corresponding to AC, 30SH-AC before and after CO_2 adsorption are ascribed

Table 3: Surface area and porosity distribution for AC and 30SH-AC.

Parameters	AC	30SH-AC
BET surface area (m^2/g)	573.26	483.91
Total pore volume (cm^3/g)	0.33	0.2744
Mean pore diameter (nm)	2.03	2.2678

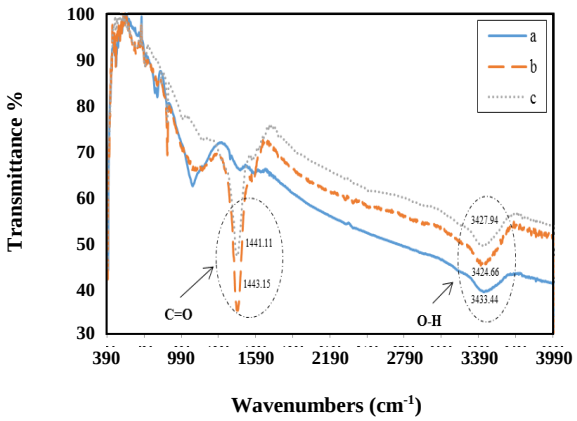

Fig. 4: FT-IR spectra for (a) AC, (b) 30SH-AC before CO_2 adsorption, (c) 30SH-AC after CO_2 adsorption.

to hydroxyl groups (-OH). Some distinct strong peaks at1443.15 and 1441.15 cm^{-1} were found on spectra of both 30SH-AC before and after CO_2 adsorption correspond to the presence of some carboxylates (C=O) which indicate that modification of activated carbon with sodium hydroxide was well done and the formation of sodium carbonate has been justified.

Response surface methodology

Generally, Response Surface Methodology (RSM) is a multivariate statistical technique used to optimize processes, i.e., to discover the conditions in which to apply a procedure in order to obtain the best possible response in the experimental region studied. This methodology involves the design of experiments and multiple regression analysis as tools to assess the effects of two or more independent variables on dependent variables. One additional advantage is the possibility of evaluating the interaction effect between the independent variables on the response. This technique is based on the fit of a polynomial equation to the experimental data to describe the behavior of a set of data [34, 35].

In this work, a standard RSM design known as Central Composite Design (CCD) was used to study the parameter for CO_2 adsorption by AC and 30SH-AC. By studying two numeric factors and one categoric factor which are: X_1, adsorption temperature (°C), X_2, adsorption pressure (bar) and X_3, kind of modifier, respectively. The CO_2 adsorption capacity and percentage were simultaneously optimized. The independent variables (X_1, X_2), their coded and actual values for optimization are presented in Table 4. Each variable was varied over five levels, -2; −1, 0, +1 and +2, at the determined ranges based on some preliminary experiments.

Temperature and pressure as two numeric factors and kind of modifier as a categorical factor at two different levels were considered as the main operating parameters. RSM was used to find the optimum of the experimental conditions. Based on the ranges and the levels given, a complete design matrix of the experiments was employed as shown in Table 5. The tests were done at least two times to confirm the reproducibility of the results.

There are 8 factorial points, 6 axial points and 6 replicates at the center points, indicated by a total of 20 experiments, as calculated from Eq. (5).

$$N = 2^n + 2n + n = 2^3 + 2\times3 + 6 = 20 \quad (5)$$

Where N is the total number of experiments required and n is the number of variables. Based on CCD design, quadratic models were developed correlating the adsorption variables to the two responses. The optimum conditions of CO_2 adsorption for 30SH-AC are: adsorption temperature (20°C) and adsorption pressure (6 bar). The CO_2 adsorption capacity and percentage obtained were 104.319 mg/g and 12%, respectively.

As can be seen in Fig. 5 (a) and (b), the experimental values for all responses were in good agreement with the amounts predicted by the RSM model both for capacity and percentage of CO_2 adsorption. Fig. 5 indicated the predicted responses obtained were more close to the experimental values due to having high R^2. In addition, the three dimensional response surfaces graphs for CO_2 adsorption capacity and percentage were depicted in Fig. 6 and Fig. 7, respectively. Figs. 6 and 7 show the effects of

Table 4: Independent numerical variables of the adsorption process (actual and coded).

Independent Variables	Unit	Symbol	Coded Level				
			-2	-1	0	+1	+2
Temperature	°C	X_1	20	35	50	65	80
Pressure	bar	X_2	2	4	6	8	10

Table 5: Experimental design matrix and results.

Run no.	T (°C)	P (bar)	Modifier	CO_2 adsorption capacity (mg/g)	CO_2 adsorption percentage (%)
	X_1	X_2	X_3	Y_1	Y_2
1	20	6	AC-NaOH	104.32	12.00
2	20	6	AC	56.89	6.57
3	35	4	AC-NaOH	55.73	10.21
4	35	4	AC	21.50	3.94
5	35	8	AC-NaOH	66.23	6.02
6	35	8	AC	38.80	3.57
7	50	2	AC-NaOH	26.63	9.81
8	50	2	AC	6.35	2.41
9	50	6	AC-NaOH	30.57	3.90
10	50	6	AC-NaOH	30.56	3.91
11	50	6	AC	9.80	1.26
12	50	6	AC	9.80	1.25
13	50	10	AC-NaOH	60.22	4.65
14	50	10	AC	40.88	3.16
15	65	4	AC-NaOH	13.75	2.72
16	65	4	AC	5.82	1.16
17	65	8	AC-NaOH	21.88	2.20
18	65	8	AC	6.95	0.70
19	80	6	AC-NaOH	12.55	1.76
20	80	6	AC	5.80	0.81

the two significant variables (X_1 and X_2) and indicate that an increase in the pressure and a decrease in temperature cause a significant enhancement in CO_2 adsorption capacity and percentage. It was observed that the maximum CO_2 adsorption capacity of 30SH-AC was achieved at the adsorption temperature of 20 °C and the pressure of 8-10 bars which are marked as red color in Fig. 6. Results revealed that CO_2 adsorption rate increases with increase in pressure while increase in temperature reduces the CO_2 adsorption capacity.

RESULTS AND DISCUSSION

Isotherm modeling

Adsorption isotherms are used to describe the surface properties and affinity of the adsorbent. Also, the performance of an adsorbent can be studied by adsorption isotherm data, which can be obtained by a series of experimental tests. Modeling the adsorption isotherm data is a needful way for predicting and comparing the adsorption performance, which is critical to optimize the adsorption mechanism pathways, for expression of

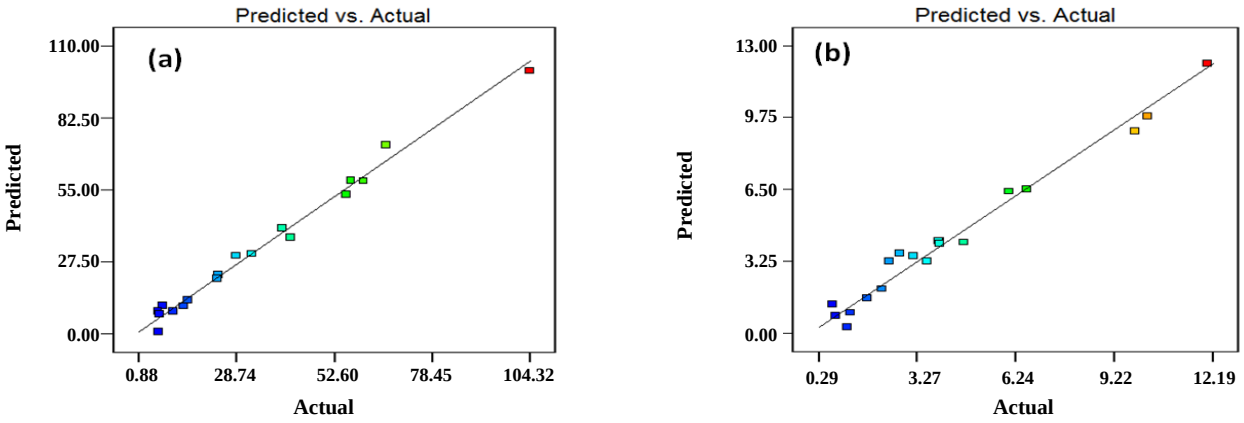

Fig. 5: Predicted vs. experimental values of CO_2 adsorption capacity (a) and of CO_2 adsorption percentage (b).

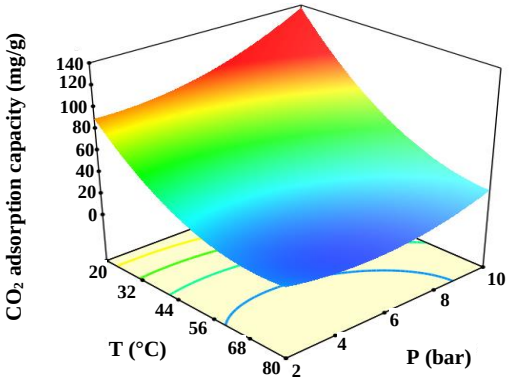

Fig. 6: Response surface plot of CO_2 adsorption capacity of 30SH-AC with temperature and pressure.

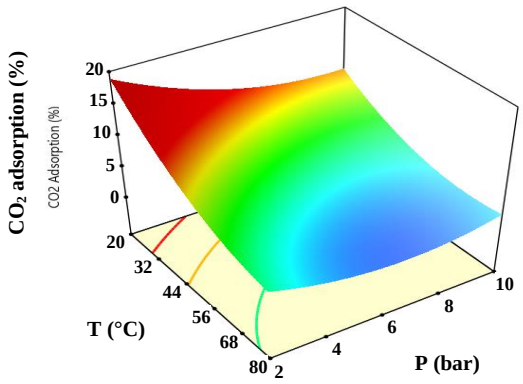

Fig. 7: Response surface plot of CO_2 adsorption percentage of 30SH-AC with temperature and pressure s.

the adsorbents capacities, and effective design of the adsorption systems [36-38].

Several isotherm models are commonly used in the modeling adsorption data, such as Langmuir, Freundlich, and Dubinin-Radushkevich. The Langmuir adsorption isotherm has been successfully used for many other real adsorption processes but more applies to adsorption on completely homogenous surfaces with the negligible interaction between adsorbed molecules [36-38]. Langmuir isotherm model is an empirical model assuming that adsorption can only occur at a finite number of definitely localized sites and considers that all surface sites have the same adsorption energy [39]. The Freundlich isotherm model is the initial known relationship describing the non-ideal and reversible adsorption, which can be applied to multilayer adsorption, on the basis of an assumption concerning the energetic surface heterogeneity. This model says that the ratio of the amount of solute adsorbed onto a given mass of sorbent to the concentration of the solute in the solution is not constant at different concentrations [36, 40]. The Dubinin-Radushkevich model is another empirical model which is formulated for the adsorption process to estimate the characteristic porosity of the biomass and the apparent energy of adsorption and it is generally applied to express the adsorption process occurred onto both homogeneous and heterogeneous surfaces [36, 39]. The Temkin isotherm is appropriate for the prediction of gas phase equilibrium. Hill's equation was postulated to explain the binding of various species onto homogeneous substrates. The model assumes that adsorption is a cooperative phenomenon, with the ligand binding ability at one site on the macromolecule, may influence different binding sites on the same macromolecule [36, 37]. The Sips adsorption isotherm model is a combined form of the Langmuir and

Table 6: Isotherm model parameters for CO_2 adsorption by 30SH-ACat 20 ℃.

No.	Models		Parameter	values
1	Langmuir	$q_e = \frac{q_m k_L P_e}{(1 + k_L P_e)}$	q_m	585.74
			K_L	0.036
			R^2	0.987
2	Freundlich	$q_e = k_F P^{1/n}$	k_F	1.146
			n	21.884
			R^2	0.985
3	Dubinin Radushkevich	$q_e = q_m e^{-\lambda\omega^2}$	q_m	130.15
			λ	1.267
			ω	0.628
			R^2	0.977
4	Temkin Model	$q_e = B \ln(AP_e)$	A	0.970
			B	57.827
			R^2	0.975
5	Hill Model	$q_e = \frac{q_s P_e^{n_H}}{K_D + P_e^{n_H}}$	q_s	167.88
			K_D	10.417
			n_H	1.564
			R^2	0.980
6	Sips Model	$q_e = \frac{K_s P_e^{\beta}}{1 + \alpha_s P_e^{\beta}}$	K_s	16.985
			β	1.462
			α_s	0.086
			R^2	0.991

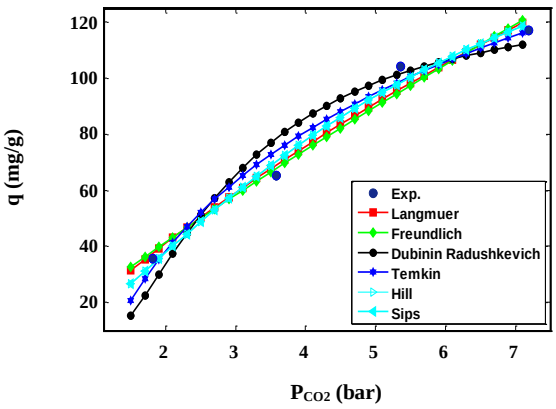

Fig. 8: Experimental equilibrium data and isotherm models for 30SH-AC.

Freundlich models [36, 41]. Fig. 8 shows the results obtained from the isothermal experiments of the 30SH-AC. The values of the isotherm constants and the correlation coefficient (R^2) of the data fittings to each of the models are shown in Table 6.

The validity of these models is evaluated by the correlation coefficient (R^2), which is within the range of 0-1, in which R^2 closer to unity implies the best fitting towards the particular isotherm model. According to the results of Table 6, the correlation coefficient (R^2) for all mentioned isotherm models is very close to 1, which indicates that the results of the experiments of this study are consistent with these 6 isotherm models.With respect to the R^2 values, the suitability of these models

Table 7: Kinetic parameters for CO_2 adsorption on 30SH-AC at pressure 6 bars.

Models		Parameter	20°C	50°C	80°C
First Order Model	$q_t = q_e\left(1-e^{(-k_f t)}\right)$	q_e	102.854	62.417	30.040
		k_f	0.0126	0.00199	0.0061
		R^2	0.975	0.957	0.970
Second Order Model	$q_t = \frac{q_e^2 k_s t}{1+q_e k_s t}$	q_e	108.213	77.012	32.810
		k_s	0.00022	0.00003	0.0003
		R^2	0.996	0.963	0.987
Ritchie Second Model	$q_t = q_e\left\{1-\left[\frac{q_e}{(1+k_2 t)}\right]\right\}$	q_e	108.2133	77.011	32.810
		k_2	0.0239	0.00221	0.010
		R^2	0.996	0.963	0.987
Elovich	$q_t = \frac{1}{\beta \ln(\alpha\beta)} + \frac{1}{\beta \ln t}$	α	0.736	0.003	0.067
		β	11.453	13.592	5.069
		R^2	0.915	0.944	0.973
Rate Controlling	$q_t = k_{id} t^{\frac{1}{2}}$	kid	3.218	1.616	0.916
		R^2	0.753	0.995	0.888

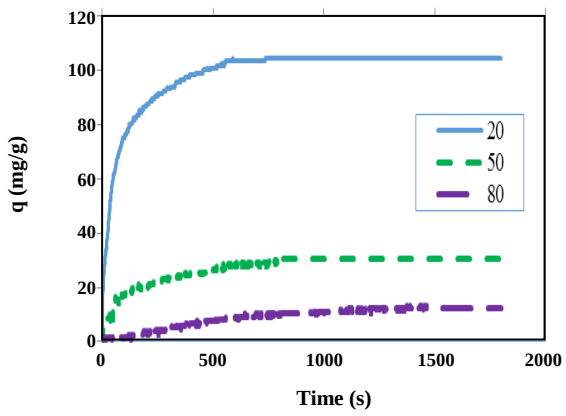

Fig. 9: Effect of Temperature on CO_2 adsorption capacity at pressure 6 bars.

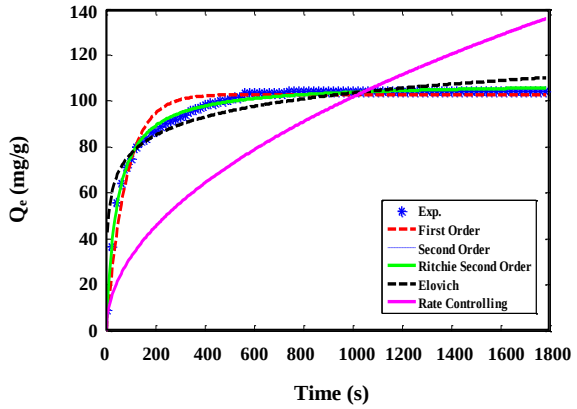

Fig. 10: Experimental kinetics adsorption and modeled kinetic adsorption for 30SH-AC.

in order of Spis > Langmuir > Frendlich > Hill > D-R > Temkin. The results revealed that the sips model with the maximum R^2 (0.991) gives the best fit of the experimental data.

Kinetics modeling

The adsorption kinetic produces valuable information about the reaction pathways and mechanism of the reactions [42, 43]. In order to find the best kinetic model to describe the adsorption of CO_2 on to 30SH-AC, the kinetic models were fitted to experimental data and their non-linear adjustments are shown in Figs. 9 and 10. In addition, the data fittings to each of the models at different temperature alongside with their correlation coefficients R^2 are presented in Table 7. The R^2 values obtained were large at all the temperature studied, and the experimental q_e values agree with the calculated values obtained from the linear plots. It can be seen that the correlation coefficients for the linear plot of the second order models at 20 °C are higher than the correlation coefficients of all other models.

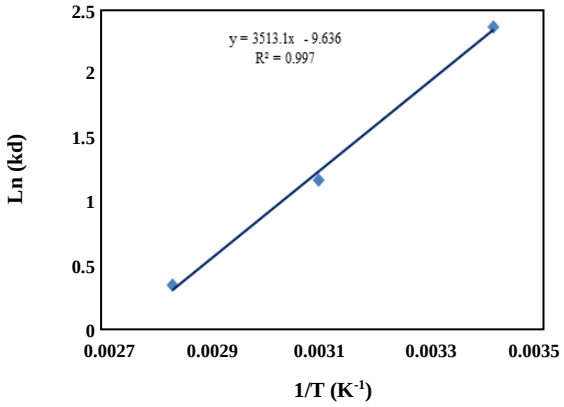

Fig. 11: Plot of Ln K_d vs. 1/T for the adsorption of CO_2 on 30SH-AC

Adsorption Thermodynamics

In engineering practice entropy and Gibbs free energy factors should be considered in order to determine what process will occur spontaneously. The thermodynamic parameters of the CO_2 adsorption process in terms of the Gibbs free energy change (ΔG°), change in Enthalpy of reaction (ΔH°), and change in entropy of adsorbate and adsorbent interaction (ΔS°) can be calculated from Van Hoff's formulation, as given in equations 6 to 8 [44].

$$\mathrm{LnK_d} = \frac{\Delta S^o}{R} - \frac{\Delta H^o}{RT} \quad (6)$$

$$K_d = \frac{P_i - P_e}{P_e} \times \frac{V}{W} 0 \quad (7)$$

$$N\Delta G^o = \Delta H^o - T\Delta S^o \quad (8)$$

The thermodynamic experiments were carried out at 20, 50 and 80 °C for gas phase pressure of 6 bars. The values of enthalpy change (ΔH°) and entropy change (ΔS°) can be determined from the slope and intercept of the plot of Ln(K_d) Vs. (1/T) respectively, which is shown in Fig. 11. The values of the thermodynamic parameters are presented in Table 8. Based on the experimental findings, the negative value in ΔH° indicates an exothermic nature of the CO_2 adsorption process, whereas negative ΔS° value suggests high orderliness of the adsorbate molecules upon adsorption. The negative ΔS° can be interpreted by the behavior of the CO_2 molecules upon the adsorption process, which is from randomized to an ordered form on the surface of the adsorbent. The reduction in the entropy value upon the adsorption process is because of a lesser degree of freedom of the gas molecule, due to minimum free space on the carbon surface. In addition, the amount of ΔH° denotes the type of CO_2 adsorption process, whether it belongs to the physical adsorption or chemical adsorption. It has been reported that the quantity of ΔH° for the physical adsorption is < 20 kJ/mol, whilst for the chemical adsorption; the value is within 20-200 kJ/mol [45, 46]. Therefore, the calculated ΔH° which is about 30 kJ/mol suggests that the CO_2 adsorption is chemisorption. The free energy value (ΔG°) for all the temperatures is negative and a decrease in the value of ΔG° with an increase in temperature shows that the reaction is easier at a low temperature. Also, the CO_2 adsorption capacity and percentage of the adsorbent decrease with increase in the temperature (Fig. 12). Fig. 11 shows that the distribution coefficient (k_d) values decreased with the rise in temperature indicating the exothermic nature of the adsorption.

Effect of adsorbent amount

As adsorbent dosage increases keeping all the other parameters at constant CO_2 adsorption capacity decreases which are shown in the Figs. 13 and 14. At lower adsorbent dosage, a number of active sites are higher. With the increase in adsorbent dosage aggregation of particles takes place, consequently, the available adsorption sites may decrease as a result CO_2 adsorption capacity decreases.

In addition, to consider the effect of mesh size variations of 30SH-AC on CO_2 adsorption, granular activated carbon was crushed and sieved through different mesh sieves (20, 35, 50 and 70) which are equal to 850, 500, 300 and 212 microns respectively. As shown in Fig. 15, it was observed that the activated carbon with a particle size of 50 mesh (300 μm) has the maximum CO_2 adsorption capacity (246.07 mg/g) which was near to activated carbon with a particle size of 35 mesh (500 μm) with 242.64 mg/g CO_2 adsorption capacity.

Temperature effect on adsorption capacity

Adsorption of CO_2 by 30SH-AC was found to be decreasing as the temperature increased 104.32, 30.56 and 12.55 mg/g for temperatures of 20, 50 and 80°C, respectively. This revealed that chemisorption of CO_2 on 30SH-AC was dominant and this was attributed to the developed porosity of the adsorbent after modification. A similar observation of better adsorption of CO_2 at a lower

Table 8: Thermodynamic parameters of CO_2 adsorption on 30SH-A

P(CO_2) (Bar)	ΔH° (kJ/mol)	ΔS° (kJ/mol.K)	ΔG°(kJ mol^{-1})		
			20 °C	50 °C	80 °C
6.000	-29.209	-0.080	-5.722	-3.319	-0.915

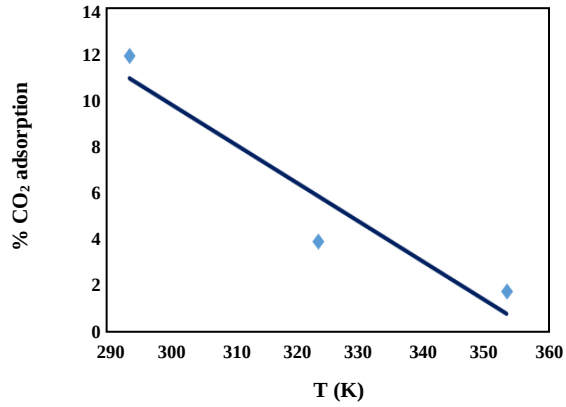

Fig. 12: Variation of CO_2 adsorption percentage with temperature.

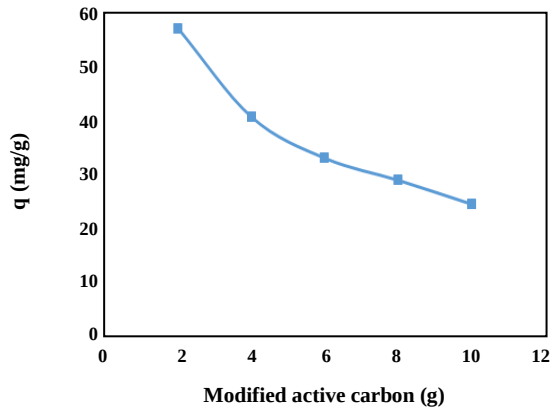

Fig. 13: The effect of adsorbent dosage on CO_2 adsorption capacity at 20°C.

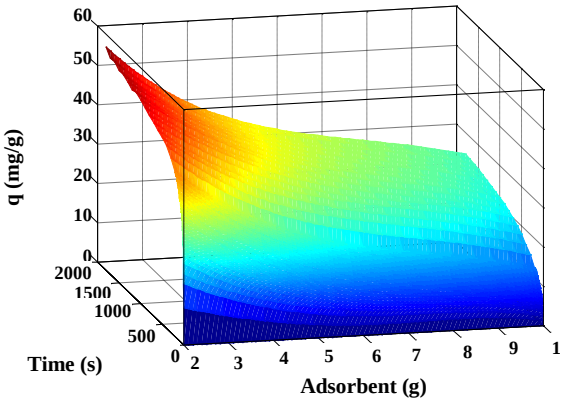

Fig. 14: The effect of time and adsorbent dosage on CO_2 adsorption capacity.

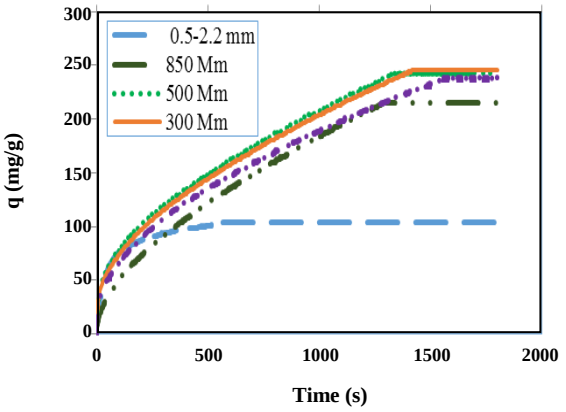

Fig. 15: Effect of mesh size variations of 30SH-AC on CO_2 adsorption.

column temperature due to the association of activated carbon with sodium and also pore size development has been reported. It can be also said that chemical adsorption activities were negated as the adsorption temperature increased.

Modification of the activated carbon with sodium hydroxide introduced some molecules of sodium on its surface which enhanced formation of sodium carbonate as CO_2 was adsorbed. The adsorption of CO_2 at different temperatures and their adsorption capacities are depicted in Fig. 16 which revealed that increasing the temperature has an inverse effect on CO_2 adsorption capacity.

Pressure effect on adsorption capacity

The effects of different adsorption pressures including 2, 4, 6 and 8 bars, on CO_2 adsorption by 30SH-AC, are presented in Figs. 17, 18 and 19. The adsorption capacity at 2 bars is 35.56 mg/g, and it gradually increases from 35.56 mg/g to 117.75 mg/g with increasing pressure from 2 to 8 bars. Fig. 19 shows the effect of pressure on CO_2 adsorption by AC and 30SH-AC. It shows that maximum adsorption capacity was carried out at 6 bars and after this pressure increasing pressure there is no impressive effect on CO_2 adsorption capacity.

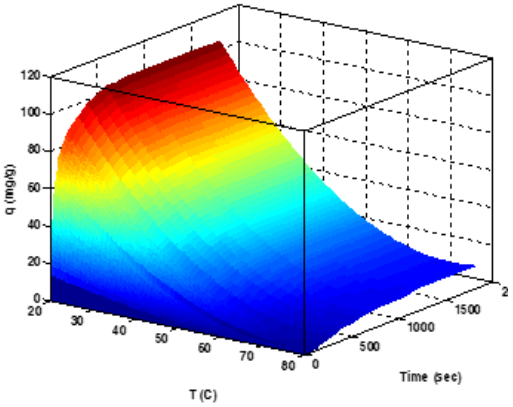

Fig. 16: Effect of time and temperature on CO_2 adsorption capacity for 30SH-AC.

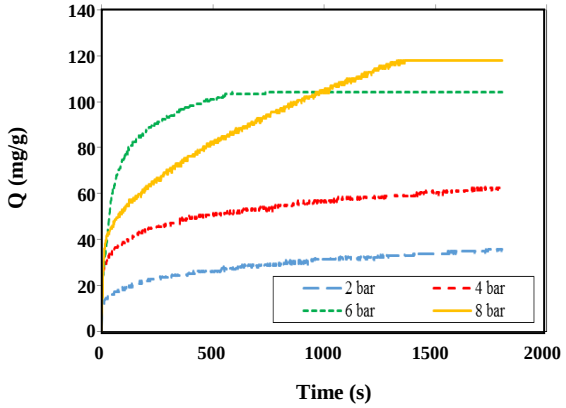

Fig. 18: The effect of pressure and time on CO_2 adsorption capacity for 30SH-AC at 20°C.

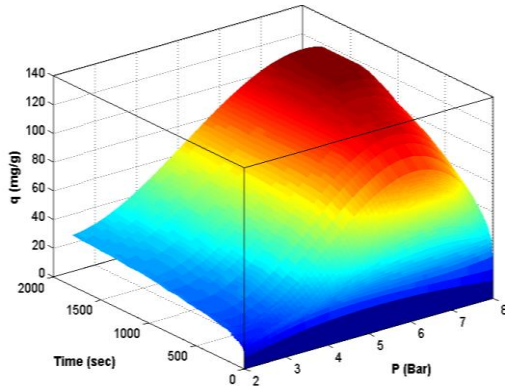

Fig. 17: The effect of time and pressure on CO_2 adsorption capacity for 30SH-AC.

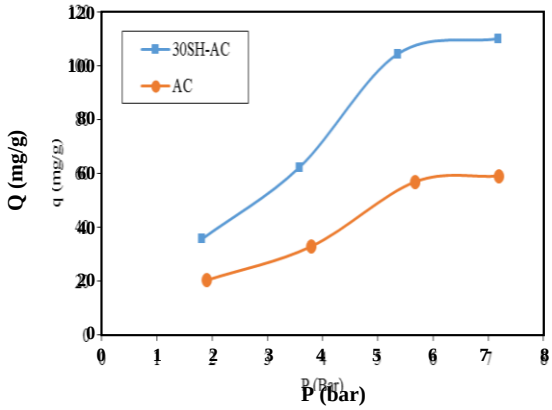

Fig. 19: The effect of pressure on equilibrium adsorption capacity for AC and 30SH-AC at 20°C.

CONCLUSIONS

Modification of activated carbon was successfully carried out with 30 % concentration of sodium hydroxide solution. The batch adsorption experiments revealed that the adsorption temperature of 20°C and 2 gr of 30SH-AC with a particle size of 50 mesh (300 µm) were suitable for the CO_2 adsorption. CO_2 adsorption capacity and CO_2 adsorption percentage were investigated using RSM. According to the obtained results, RSM was an adequately applicable method for optimizing the operating variables for the CO_2 adsorption process. In addition, the results showed very high coefficients of the determination values ($R^2 > 0.99$), confirming that the experimental data fitted well into the data. Moreover, the pressure had a positive effect on the CO_2 adsorption capacity which means that CO_2 adsorption capacity increases with increase in pressure while the increase in temperature reduces the adsorption capacity. Further, experimental results were analyzed through the adsorption isotherm models. It was found that the Sips model can satisfactorily describe the experimental isotherm data of CO_2 adsorption on the 30SH-AC. Besides, the kinetic analysis demonstrated that the CO_2 adsorption onto the 30SH-AC obeys the pseudo-second-order model and the thermodynamics parameters showed that the CO_2 adsorption process is exothermic in nature.

Nomenclature

K_L	Langmuir constant, bar^{-1}
k_F	Freundlich constant, $cm^3/g.bar^{1/n}$
k_T	Temkin constant, $cm^3/g.bar$
K_D	Hill constant
K_s	Sips constant

k_f	Rate constant of pseudo-first order adssorption, min^{-1}
k_s	Rate constant of the pseudo-second order kinetics, g/mg.min
k_2	Reaction rate constant of Ritchie second order equation, min^{-1}
k_{id}	Intraparticle diffusion rate constant, mg/g.min
M_{CO2}	Molar mass of carbon dioxide, g/mol
m	Mass of adsorbent, g
N	Total number of experiments required
n	Number of variables
n_H	Hill cooperativity coefficient of the binding interaction
P_i	Initial pressure, bar
P_e	Equilibrium pressure, bar
q_e	Equilibrium adsorption capacity, mg/g, cm^3/g
$\bar{q}_e$	Average of q_e, mg/g
q_m	Maximum CO_2 adsorption capacity, cm^3/g
q_s	Hill isotherm maximum uptake saturation, mg/L
q_t	Amount of adsorbed CO_2 at time t,
R	Universal gas constant, 8.314 J/mol.K
R^2	Correlation coefficient
R_L	Dimensionless constant
T	Temperature of the reactor, K
t	Reaction time, min
V	Volume of the reactor occupied by the CO_2 gas, mL
W	Grams of adsorbent, g

Greek Letters

α	Initial adsorption rate, mg/g.min
β	Desorption constant, g/mg
λ	D-R constant, mol^2/J^2
ω	Polanyi potential (equivalent to RT ln (1/1+P))
ΔH°	Enthalpy change, kJ/mol
ΔS°	Entropy change, kJ/mol.K
ΔG°	Gibbs free energy change, kJ/mol

Received : Jul. 26, 2018 ; Accepted :Oct. 8, 2018

REFERENCES

[1] Pashaei H., Ghaemi A., Nasiri M., Modeling and Experimental Study on the Solubility and Mass Transfer of CO_2 into Aqueous DEA Solution Using a Stirrer Bubble Column, *RSC Advances*, **6**(109): 108075-108092 (2016).

[2] Hajilary N., Rezakazemi M., CFD Modeling of CO_2 Capture by Water-Based Nanofluids Using Hollow Fiber Membrane Contactor, *International Journal of Greenhouse Gas Control*, **77**: 88-95 (2018).

[3] Norouzbahari S., Shahhosseini S., Ghaemi A., Modeling of CO_2 Loading in Aqueous Solutions of Piperazine: Application of an Enhanced Artificial Neural Network Algorithm, *Journal of Natural Gas Science and Engineering*, **24**:18-25 (2015).

[4] Ghaemi A., Shahhosseini Sh, Ghannadi Maragheh M., Experimental Investigation of Reactive Absorption of Ammonia and Carbon Dioxide by Carbonated Ammonia Solution, *Iraian Journal of Chemistry and chemical Engineering (IJCCE)*, **30**(2): 43-50 (2011).

[5] Shirazian S., Marjani A., Rezakazemi M., Separation of CO_2 by Single and Mixed Aqueous Amine Solvents in Membrane Contactors: Fluid Flow and Mass Transfer Modeling, *Engineering with Computers*, **28**(2): 189-198 (2012).

[6] Rezakazemi M., Sadrzadeh M., Matsuura T., Thermally Stable Polymers for Advanced High-Performance Gas Separation Membranes, *Progress in Energy and Combustion Science*, **66**: 1-41 (2018).

[7] Zhang Z., Chen F., Rezakazemi M., Zhang W., Lu C., Chang H., Quan X., Modeling of a CO_2-Piperazine-Membrane Absorption System, *Chemical Engineering Research and Design*, **131**: 375-84 (2018).

[8] Rezakazemi M., Khajeh A., Mesbah M., Membrane Filtration of Wastewater From Gas and Oil Production, *Environmental Chemistry Letters*, **16**, 367-388 (2018).

[9] Norouzbahari S., Shahhosseini S., Ghaemi A., Chemical Absorption of CO_2 into an Aqueous Piperazine (PZ) Solution: Development and Validation of a Rigorous Dynamic Rate-Based Model, *RSC Advances*, **6**(46): 40017-40032 (2016).

[10] Razavi SMR., Rezakazemi M., Albadarin AB., Shirazian S., Simulation of CO_2 Absorption by Solution of Ammonium Ionic Liquid in Hollow-Fiber Contactors, *Chemical Engineering and Processing: Process Intensification*, **108**: 27-34 (2016).

[11] Norouzbahari S., Shahhosseini S., Ghaemi A., CO_2 Chemical Absorption Into Aqueous Solutions of Piperazine: Modeling of Kinetics and Mass Transfer Rate, *Journal of Natural Gas Science and Engineering*, **26**: 1059-1067 (2015).

[12] Gao J., Yin J., Zhu F., Chen X., Tong M., Kang W., Zhou Y., Lu J., Experimental Study of a Hybrid Solvent MEA-Methanol for Post-Combustion CO_2 Absorption in an Absorber Packed with Three Different Packing: Sulzer BX500, Mellapale Y500, Pall Rings 16× 16, *Separation and Purification Technology*, **163**: 23-29 (2016).

[13] Rezakazemi M., Heydari I., Zhang Z., Hybrid Systems: Combining Membrane and Absorption Technologies Leads to More Efficient Acid Gases (CO_2 and H_2S) Removal from Natural Gas, *Journal of CO_2 Utilization*, **18**: 362-369 (2017).

[14] Wang L., Yao M., Hu X., Hu G., Lu J., Luo M., Fan M., Amine-Modified Ordered Mesoporous Silica: The Effect of Pore Size on CO_2 Capture Performance, *Applied Surface Science*, **324**: 286-292 (2015).

[15] Rezakazemi M., Niazi Z., Mirfendereski M., Shirazian S., Mohammadi T., Pak A., CFD Simulation of Natural Gas Sweetening in a Gas–Liquid Hollow-Fiber Membrane Contactor, *Chemical Engineering Journal*, **168**(3): 1217-1226 (2011).

[16] Díez N., Álvarez P., Granda M., Blanco C., Santamaría R., Menéndez R., CO_2 Aadsorption Capacity and Kinetics in Nitrogen-Enriched Activated Carbon Fibers Prepared by Different Methods, *Chemical Engineering Journal*, **281**: 704-712 (2015).

[17] Yu C-H., Huang C-H., Tan C-S., A Review of CO_2 Capture by Absorption and Adsorption, *Aerosol Air Qual. Res*, **12**(5): 745-769 (2012).

[18] Tan Y., Islam M.A., Asif M., Hameed B., Adsorption of Carbon Dioxide by Sodium Hydroxide-Modified Granular Coconut Shell Activated Carbon in a Fixed Bed, *Energy*, **77**: 926-931 (2014).

[19] Foroutan R., Esmaeili H., Abbasi M., Rezakazemi M., Mesbah M., Adsorption Behavior of Cu (II) and Co (II) Using Chemically Modified Marine Algae, *Environmental Technology*, **39**(21): 2792-2800 (2018).

[20] Dali AM., Ibrahem AS., Hadi A., General Study About Activated Carbon for Adsorption Carbon Dioxide, *Journal of Purity, Utility Reaction and Environment*, **1**(5): 236-251 (2012).

[21] Somy A., Mehrnia MR., Amrei HD., Ghanizadeh A., Safari M., Adsorption of Carbon Dioxide Using Impregnated Activated Carbon Promoted by Zinc, *International Journal of Greenhouse Gas Control*, **3**(3): 249-254 (2009) .

[22] Lee S-Y., Park S-J., A Review on Solid Adsorbents for Carbon Dioxide Capture, *Journal of Industrial and Engineering Chemistry*, **23**: 1-11 (2015).

[23] Mirzaeian M., Hall P., Thermodynamical Studies of Irreversible Sorption of CO_2 by Wyodak Coal, *Iraian Journal of Chemistry and Chemical Engineering (IJCCE)*, **27**(2): 59-68 (2008).

[24] Noorpoor A., Nazari Kudahi S., Mahmoodi N.M., Adsorption Performance Indicator for Power Plant CO_2 Capture on Graphene Oxide/TiO_2 Nanocomposite, *Iranian Journal of Chemistry and Chemical Engineering (IJCCE)*, **38**(3): 293-307 (2019).

[25] Samanta A., Zhao A., Shimizu GK., Sarkar P., Gupta R., Post-Combustion CO_2 Capture Using Solid Sorbents: A Review, *Industrial & Engineering Chemistry Research*, **51**(4): 1438-1463 (2011).

[26] Auta M., Darbis N.A., Din A.M., Hameed B., Fixed-Bed Column Adsorption of Carbon Dioxide by Sodium Hydroxide Modified Activated Alumina, *Chemical Engineering Journal*, **233**: 80-87 (2013).

[27] Buczek B., Preparation of Active Carbon by Additional Activation with Potassium Hydroxide and Characterization of Their Properties, *Advances in Materials Science and Engineering*, **2016**, (2016).

[28] Guo B., Chang L., Xie K., Adsorption of Carbon Dioxide on Activated Carbon, *Journal of Natural Gas Chemistry*, **15**(3): 223-229 (2006).

[29] Shahkarami S., Azargohar R., Dalai A.K., Soltan J., Breakthrough CO_2 Adsorption in Bio-Based Activated Carbons, *Journal of Environmental Sciences*, **34**: 68-76 (2015).

[30] Sreńscek-Nazzal J., Narkiewicz U., Morawski A., Wróbel R., Gęsikiewicz-Puchalska A., Michalkiewicz B., Modification of Commercial Activated Carbons for CO_2 Adsorption, *Acta Physica Polonica, A*, **129** (3), (2016).

[31] Jaunsen J.R., "The Behavior and Capabilities of Lithium Hydroxide Carbon Dioxide Scrubbers in a Deep Sea Environment", Naval Academy Annapolis Md, (1989).

[32] Saeidi M., Ghaemi A., Tahvildari K., Derakhshi P., Exploiting Response Surface Methodology (RSM) as a Novel Approach for the Optimization of Carbon Dioxide Adsorption by Dry Sodium Hydroxide, *Journal of the Chinese Chemical Society*, **65**(12): 1465-1475 (2018).

[33] Chen J.H., Wong D.S.H., Tan C.S., Subramanian R., Lira C.T., Orth M., Adsorption and Desorption of Carbon Dioxide onto and from Activated Carbon at High Pressures, *Industrial & Engineering Chemistry Research*, **36**(7): 2808-2815 (1997).

[34] Khalili S., Khoshandam B., Jahanshahi M., Optimization of Production Conditions for Synthesis of Chemically Activated Carbon Produced from Pine Cone Using Response Surface Methodology for CO_2 Adsorption, *RSC Advances*, **5**(114): 94115-94129 (2015).

[35] Amiri M., Shahhosseini S., Ghaemi A., Optimization of CO_2 Capture Process from Simulated Flue Gas by Dry Regenerable Alkali Metal Carbonate Based Adsorbent Using Response Surface Methodology, *Energy & Fuels*, **31**(5): 5286-5296 (2017).

[36] Chen X., Modeling of Experimental Adsorption Isotherm Data, *Information*, **6**(1):14-22 (2015).

[37] Gaurina-Medjimurec N., "Handbook of Research on Advancements in Environmental Engineering", *IGI Global*, (2014).

[38] Rashidi NA., Yusup S., Borhan A., Isotherm and Thermodynamic Analysis of Carbon Dioxide on Activated Carbon, *Procedia Engineering*, **148**: 630-637 (2016).

[39] Singh VK., Kumar EA., Measurement and Analysis of Adsorption Isotherms of CO_2 on Activated Carbon, *Applied Thermal Engineering*, **97**: 77-86 (2016).

[40] Freundlich H., Über Die Adsorption in Lösungen, *Zeitschrift für Physikalische Chemie*, **57**(1): 385-470 (1907).

[41] Arjmandi M., Pakizeh M., An Experimental Study of H_2 And CO_2 Adsorption Behavior of C-MOF-5 And T-MOF-5: A Complementary Study, *Brazilian Journal of Chemical Engineering*, **33**(1): 225-233 (2016).

[42] Çağlayan B.S., Aksoylu A.E., CO_2 Adsorption Behavior and Kinetics on Chemically Modified Activated Carbons, *Turkish Journal of Chemistry*, **40**(4): 576-587 (2016).

[43] Ejikeme P., Ejikeme EM., Okonkwo GN., Equilibrium, Kinetic and Thermodynamic Studies on Basic Dye Adsorption Using Composite Activated Carbon, *International Journal of Technical Research and Applications*, **2**: 96-103 (2014).

[44] Cen Q., Fang M., Wang T., Majchrzak-Kucęba I., Wawrzyńczak D., Luo Z., Thermodynamics and Regeneration Studies of CO_2 Adsorption on Activated Carbon, *Greenhouse Gases: Science and Technology*, **6**(6): 787-796 (2016).

[45] Zhao Y., Wang D., Xie H., Won SW., Cui L., Wu G., Adsorption of Ag (I) from Aqueous Solution by Waste Yeast: Kinetic, Equilibrium and Mechanism Studies, *Bioprocess and Biosystems Engineering*, **38**(1): 69-77 (2015).

[46] Liang S., Guo X., Feng N., Tian Q., Isotherms, Kinetics and Thermodynamic Studies of Adsorption of Cu^{2+} from Aqueous Solutions by Mg^{2+}/K^{+} Type Orange Peel Adsorbents, *Journal of Hazardous Materials*, **174**(1): 756-762 (2010)